A RUNGE-KUTTA METHOD WITH USING EIGHTH-ORDER NEARLY-ANALYTIC SPATIAL DISCRETIZATION OPERATOR FOR SOLVING A 2D ACOUSTIC WAVE EQUATION

CHAOYUAN ZHANG[1,2], XIAO LI[2], XIAO MA[2] and GUOJIE SONG[3]

[1] *College of Mathematics and Computer, Dali University, Dali 671003, P.R. China. zcy_km@163.com*
[2] *Department of Mathematical Sciences, Tsinghua University, Beijing 100084, P.R. China.*
[3] *Department of Computer Science and Technology, Tsinghua University, Beijing 100084, P.R. China.*

(Received March 12, 2013; revised version accepted May 6, 2014)

ABSTRACT

Zhang, C., Li, X., Ma, X. and Song, G., 2014. A Runge-Kutta method with using eighth-order nearly-analytic spatial discretization operator for solving a 2D acoustic wave equation. *Journal of Seismic Exploration*, 23: 279-302.

In this paper, we develop an eighth-order NAD-RK method for solving a 2D acoustic wave equation. The new method uses an eighth-order nearly-analytic discretization (NAD) operator to approximate the high-order spatial derivatives in the wave equation. The wavefield displacements and their gradients are used simultaneously. And we apply a third-order Runge-Kutta (RK) method to solve the semi-discrete ordinary differential equations (ODEs) with respect to time. Thus this method has third-order accuracy in time and can achieve eighth-order accuracy in space. Theoretical properties including stability and errors are analyzed for the eighth-order NAD-RK method in detail. Meanwhile, the numerical dispersion relationship for this method is investigated and the numerical dispersion is tested in our study. The study shows that the eighth-order NAD-RK method has the smallest numerical dispersion and the weakest numerical dispersion anisotropy compared with the eighth-order Lax-Wendroff correction (LWC) method and the eighth-order staggered-grid (SG) method. The computational efficiency of the eighth-order NAD-RK method is also tested. The results show that the eighth-order NAD-RK method needs less computational time and requires less memory than the eighth-order LWC and SG methods. Finally, the eighth-order NAD-RK method is used to simulate acoustic wavefields for two heterogeneous layered models. The simulation results further demonstrate that the eighth-order NAD-RK method can provide high-order accuracy for the complex heterogeneous models and is effective to suppress the numerical dispersion caused by discretizing the acoustic wave equation when too coarse grids are used or strong discontinuities exist in the medium. Thus, the eighth-order NAD-RK method can be potentially used in seismic tomography and large-scale wave propagation problems.

KEY WORDS: RK method, numerical dispersion, acoustic wave equation, NAD operator.

0963-0651/14/$5.00

INTRODUCTION

Numerical methods for solving wave equations have been playing an important role in exploration seismology. The previous numerical models are mainly used as an interpretive aid in complex geology and as a benchmark for testing algorithms. With a great increase of computer performance and memory, plenty of numerical methods are proposed to simulate wave phenomena in the complex media and widely applied in waveform inversion of earth structure. However, the quality of a numerical method depends heavily on the accuracy resolution for a wide range of temporal and spatial increments present in acoustics and seismology. Therefore, it is important to develop efficient numerical method with high accuracy and fast computation speed.

At present, the main numerical methods for solving the seismic wave equations include the finite-element method (Chen, 1984; Ma and Liu, 2006; Moczo et al., 2007; Smith, 1975; Yang 2002), the pseudo-spectral method (Huang, 1992; Kelly and Marfurt, 1990; Kosloff and Baysal, 1982; Kosloff et al., 1984; Marfurt, 1984), the finite-difference method (Dablain, 1986; Dong et al., 2000; Kelly and Wave, 1976; Lele, 1992; Moczo et al., 2000, 2002; Saenger et al., 2000), the reflectivity method (Chen, 1993), the spectral element method (Komatitsch and Vilotte, 1998; Seriani and Priolo, 1994), and so on. The advantages and disadvantages of those methods have been discussed and analyzed in the cited references (Chen et al., 2010; Yang et al., 2007, 2012, 2010). As we all know, finite difference (FD) is the most widely used numerical scheme in solving the wave equation for wave propagation in seismology due to easy implementation. A low-order FD method on the temporal derivatives is effective and stable, however, this limits the accuracy of modeling. To increase the simulation accuracy, the high-order FD methods (Blanch and Robertson, 1997; Lax and Wendroff, 1964; Virieux, 1986; Zeng and Liu, 2001) have been proposed on the spatial derivatives, such as the high-order Lax-Wendroff correction (LWC) method and the high-order displacement-stress staggered-grid (SG) FD method. Unfortunately, the high-order FD methods are usually unstable in the wavefield modeling (Chen, 2007) and often have very large numerical dispersions (Yang et al., 2002, 2006; Zhang et al., 1999; Zheng et al., 2006) resulting from the discretization of wave equations when too few samples per wavelength are used or strong interfaces exist in the model. In the last years, the so-called time-space domain FD methods (Finkelstein and Kästner, 2007, 2008) have been proposed to calculate the seismic wave propagation in time and space domain. A new time-space domain high-order FD method has been developed by Liu and Sen (2009) and successfully applied to model the acoustic wavefields propagation. But the unified methodologies generally decrease the modeling accuracy with the increasing of the wavenumber and still suffer from serious numerical dispersions when models have large velocity contrasts between different layers.

In recent years, the nearly-analytic discrete (NAD) method (Yang et al., 2003) and various NAD-type methods (Wang et al., 2009; Yang et al., 2006, 2007, 2009) have been developed to effectively suppress the numerical dispersion caused by discretizing the seismic wave equations when too coarse grids are used. Based on the truncated Taylor series expansion and local interpolation compensation for the truncated Taylor series, the NAD method uses the linear combinations of a function and its spatial gradients to approximate the high-order spatial derivatives, leading to preservation of more wavefield information and a more compact spatial discretization. Plenty of detailed discussions of NAD-type methods are available in references (Wang et al., 2009; Yang et al., 2006, 2007, 2009). These NAD-type methods are much better at suppressing numerical dispersion than the FD methods above. But the spatial accuracy of these methods is only 4th-order, the research on NAD operator with higher-order accuracy is needed.

In this paper, we propose an alternative numerical method combining the Runge-Kutta method with high-order nearly-analytic discretization operators for solving 2D acoustic wave equation in order to further reduce the numerical dispersion, which is called the eighth-order NAD-RK method in brief. We first transform the 2D acoustic wave equations into an semi-discrete ordinary differential equations (ODEs) and solve the converted ODEs by using the third-order RK method (Qiu et al., 2008), which is a very stable and effective numerical computational method for solving the ODEs. Then we use the eighth-order nearly-analytic discretizations (Tong et al., 2013) to approximate the second- and third-order spatial derivatives included in the converted ODEs. Meanwhile, we analyze the stability condition, theoretical error, numerical error, numerical dispersion relation, and computational efficiency for the 2D acoustic case. Numerical results show that the eighth-order NAD-RK method can significantly suppress numerical dispersion, greatly shorten the CPU time, and reduce memory usage, compared with the SG method with an accuracy of $O(\Delta t^2 + \Delta x^8 + \Delta z^8)$ (simply called the eighth-order SG method hereafter) and the LWC method with an accuracy of $O(\Delta t^4 + \Delta x^8 + \Delta z^8)$ (called the eighth-order LWC method). Finally, the wavefields modeling results show that the eighth-order NAD-RK method can provide higher accuracy solution than the eighth-order LWC method, the eighth-order SG method and the new time-space domain high-order FD method with an accuracy of $O(\Delta t^2 + \Delta x^8 + \Delta z^8)$ (called the eighth-order TSD-FD method).

FORMULATION OF THE EIGHTH-ORDER NAD-RK METHOD

As we know, any numerical method for solving the seismic wave equations involves the approximations of the spatial derivatives and temporal derivatives. In conventional FD methods such as LWC method and SG method, the temporal derivatives included in the wave equations are approximated by the

truncated Taylor series expansion, and the spatial derivatives are approximated using the linear combinations of displacements at some grid point and its neighboring grid points. In conventional NAD-type methods, the high-order spatial derivatives are approximated using the fourth-order NAD operators. In this section, by using the third-order Runge-Kutta method to discretize the time derivatives and the eighth-order NAD operators to approximate the high-order spatial derivatives, we develop an eighth-order NAD-RK method, which uses both wavefield displacements information and gradient field information to reconstruct wavefield of the displacements. In other words, in the eighth-order NAD-RK method, we use simultaneously wave displacements and their gradients to approximate the high-order derivatives included in wave equations.

To derive the eighth-order NAD-RK method, firstly we briefly review the third-order Runge-Kutta method for solving ODE.

Third-order Runge-Kutta method for solving ODE

Consider the following ordinary differential equation

$$du/dt = L(u) \quad , \tag{1}$$

where $u = u(x,t)$, with $x \in R^2$ denoting space variables and t denoting time variable, and $L(u)$ is a known function with respect to u. We can numerically solve eq. (1) as an ordinary equation using the following third-order Runge-Kutta method (Qiu et al., 2008)

$$\begin{cases} u^{(1)} = u^n + (1/3)\Delta t L(u^n) \quad , \\ u^{(2)} = u^n + (2/3)\Delta t L(u^{(1)}) \quad , \\ u^{n+1} = \frac{1}{4}u^n + (3/4)u^{(1)} + (3/4)\Delta t L(u^{(2)}) \quad , \end{cases} \tag{2}$$

where Δt is the time step, $u^{(1)}$ and $u^{(2)}$ are intermediate variables, and $u^n = u(n\Delta t)$.

Of course, we can also use the fourth-order Runge-Kutta method to solve eq. (1). However, it will inevitably increase the computational cost and storage space.

To save storage space and improve calculation speed, by eliminating the intermediate variables of $u^{(1)}$ and $u^{(2)}$ in scheme (2), we can obtain the computational formula as follows

$$u^{n+1} = u^n + \Delta t L(u^n) + (1/2)\Delta t^2 L^2(u^n) + (1/6)\Delta t^3 L^3(u^n) \quad . \tag{3}$$

To use the third-order Runge-Kutta method for solving the acoustic wave equation, we need to transform the acoustic wave equation.

Transforms of acoustic wave equation

The 2D acoustic wave equation in a homogeneous medium is given by

$$\partial^2 u/\partial t^2 = c_0^2[(\partial^2 u/\partial x^2) + (\partial^2 u/\partial z^2)] \quad , \tag{4}$$

where u is the displacement and c_0 is the acoustic velocity.

Let $w = \partial u/\partial t$, $U = [u,(\partial u/\partial x),(\partial u/\partial z)]^T$, $W = [w,(\partial w/\partial x),(\partial w/\partial z)]^T$. From eq. (4), we can obtain the following vector equations

$$\begin{cases} \partial U/\partial t = W \quad , \\ \partial W/\partial t = A \cdot U \quad , \end{cases} \tag{5}$$

where the third-order spatial differential operator A is defined by $A = c_0^2[(\partial^2/\partial x^2) + (\partial^2/\partial z^2)]I_{3x3}$, with I_{3x3} a 3 x 3 identity matrix. Let $V = (U,W)^T$, then eq. (5) can be rewritten as follows

$$\partial V/\partial t = L \cdot V \quad , \tag{6}$$

where the spatial differential operator L is defined by $L = \begin{pmatrix} 0 & I_{3x3} \\ A & 0 \end{pmatrix}_{6x6}$.

Eighth-order NAD-RK method

Apparently, eq. (6) is a system of ODEs, so we consider to solve it by the idea of solving ODEs. Following, we will take two steps to solve eq. (6).

First, we use the local interpolation method (Yang et al., 2003) to approximate the second- and third-order spatial derivatives of displacement u and particle-velocity w in the right-hand side of eq. (6), by the linear combinations of u,w, and their spatial gradients at the grid point (i,j) and their neighboring grid points. These computational formulae of the high order nearly-analytic operator (Tong et al., 2013) for approximating the second- and third-order derivatives are listed in Appedix A for detail. Here, because we simultaneously use the wave-displacement, particle-velocity, and their gradients to reconstruct the wave-displacement and velocity fields, the eighth-order NAD-RK method can work very well in reducing the numerical dispersion even when the strong discontinuity exists in complex media or the coarse spatial step is used.

Second, after the high-order derivatives are discretized, eq. (6) is converted into a system of semi-discrete ODEs with respect to t and can be solved by the third-order Runge-Kutta method [formula (3)]. In other words, we can apply formula (3) to solve the semi-discrete ODEs (6) as follows

$$V^{n+1} = V^n + \Delta t L(V^n) + + (1/2)\Delta t^2 L^2(V^n) + (1/6)\Delta t^3 L^3(V^n) \quad . \tag{7}$$

where $V^n = V(n\Delta t)$. Substituting $V = (U,W)^T$ into eq. (7), we can obtain the computational formulae as follows

$$U^{n+1} = U^n + \Delta t W^n + (1/2)\Delta t^2 A(U^n) + (1/6)\Delta t^3 A(W^n) \quad , \tag{8a}$$

$$W^{n+1} = W^n + \Delta t A(U^n) + (1/2)\Delta t^2 A(W^n) + (1/6)\Delta t^3 A^2(U^n) \quad , \tag{8b}$$

where $A = c_0^2[(\partial^2/\partial x^2) + (\partial^2/\partial z^2)]I_{3x3}$ and $A^2 = A \cdot A$.

Eqs. (8a) and (8b) are called the eighth-order NAD-RK method.

STABILITY CRITERION AND ERROR ANALYSIS

Stability criterion

In order to keep numerical iterations stable, we need to consider how to choose the appropriate time and space steps, i.e. Δt, Δx and Δz. As we know, the Courant number α defined by $\alpha = c_0\Delta t/h$, under the condition $\Delta x = \Delta z = h$, mathematically gives the relationship between the velocity c_0 and the two grid sizes. We need to decide the range of α to make our method stable. In this section we derive the stability condition of the eighth-order NAD-RK method for the 2D case. Following the Fourier analysis and the analysis process proposed by Yang et al. (2006), after a series of mathematical operations (see Appedix B), we obtain the following stability condition for the 2D case:

$$\Delta t \leq \alpha_{max}(h/c_0) \approx 0.5416(h/c_0) \quad , \tag{9}$$

where α_{max} is the maximum value of the Courant number.

Error analysis

Using the Taylor series expansion, it can be shown that the errors of the interpolation formulae presented in Appendix A for $\partial^{m+l}u/\partial x^m \partial z^l$ ($2 \leq m+l \leq 3$) are $O(\Delta x^8 + \Delta x^8)$. In other words, the eighth-order NAD-RK method is an eighth-order accuracy scheme in space. When the third-order Runge-Kutta method is used to solve the ODEs (6), the temporal derivative error should be

$O(\Delta t^3)$. Therefore, the theoretical error of the eighth-order NAD-RK method is $O(\Delta t^3 + \Delta x^8 + \Delta z^8)$.

In the following we investigate the numerical errors of the eighth-order NAD-RK method. We consider the following 2D initial value problem

$$\begin{cases} \partial^2 u/\partial t^2 = c_0^2[(\partial^2 u/\partial x^2) + (\partial^2 u/\partial z^2)] \ , \\ u(0,x,z) = \cos[2\pi f_0\{-(\cos\theta_0/c_0)x - (\sin\theta_0/c_0)z\}] \ , \\ \partial u(0,x,z)/\partial t = -2\pi f_0 \sin[2\pi f_0\{-(\cos\theta_0/c_0)x - (\sin\theta_0/c_0)z\}] \ , \end{cases} \tag{10}$$

where θ_0 is the incident angle at time $t = 0$ and f_0 is the frequency. The exact solution of this initial value problem (10) is given analytically by

$$u(t,x,z) = \cos[2\pi f_0\{t - (\cos\theta_0/c_0)x - (\sin\theta_0/c_0)z\}] \ . \tag{11}$$

The relative numerical error is defined as follows

$$E_r(\%) = \sqrt{\{\sum_{i=1}^{N}\sum_{j=1}^{M}[u(t_n,x_i,z_j) - u_{i,j}^n]^2 / \sum_{i=1}^{N}\sum_{j=1}^{M}[u(t_n,x_i,z_j)]^2\}} \times 100\% \ , \tag{12}$$

where $u(t_n,x_i,z_j)$ is the exact solution and $u_{i,j}^n$ is the numerical solution.

In the numerical experiment, the computational parameters are chosen by the computational domain $0 < x,z \leq 10$ km, frequency $f_0 = 20$ Hz, acoustic velocity $c_0 = 4$ km/s, grid sizes $\Delta x = \Delta z = 50$ m, and the time step $\Delta t = 0.001$ s. Fig. 1 shows the computational results of the relative error $E_r(\%)$ as given in eq. (12). Three curves correspond to the eighth-order NAD-RK method, the eighth-order LWC method, and the eighth-order SG method, respectively. From Fig. 1, we can observe that the eighth-order NAD-RK method has the smallest numerical error among the three numerical methods.

NUMERICAL DISPERSION

In this section we analyze the numerical dispersion relation of the eighth-order NAD-RK method for the 2D acoustic wave equation (see Appendix C), following the methods proposed in by Yang et al. (2012) and Dablain (1986).

Dispersion relations (C-2) and (C-3) show that the numerical dispersion of the eighth-order NAD-RK method is a non-linear function of the propagation

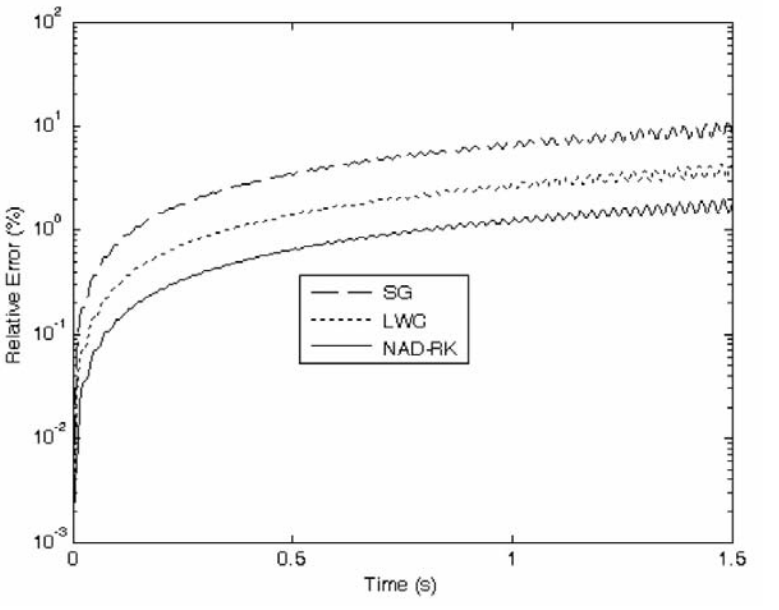

Fig. 1. The relative errors of the eighth-order NAD-RK method, the eighth-order LWC method, and the eighth-order SG method measured by E_r, are shown in a semi-log scale for the 2D initial value problem (10). Here, the spatial and temporal increments are 50 m and 1 ms, respectively. angle

θ and the Courant number α. Thus we choose the wave propagating azimuths of $\theta = 0°, 15°, 30°, 45°$ to investigate the effect of wave propagation directions on the numerical dispersion for the 2D case and compare the eighth-order NAD-RK method against the eighth-order LWC method and the eighth-order SG method.

Fig. 2 shows the variation of numerical dispersion errors along with the sampling ratio S. Four curves shown in Fig. 2 denote different propagation directions $\theta = 0°, 15°, 30°, 45°$, respectively. Here, the curve farther deviates from R = 1, means that the numerical dispersion error is greater. Table 1 gives the maximum dispersion errors in different wave propagation directions for three methods at different Courant numbers. Table 2 shows the maximum differences of the maximum dispersion errors in different wave propagation directions for three methods at different Courant numbers. The curves plotted in Figs. 2(a)-(c) are the numerical dispersion ratio of the eighth-order NAD-RK method for the Courant numbers 0.1, 0.3, and 0.4, respectively. Figs. 2(a)-(c) show that the maximum phase velocity error is about 7.42% (See Table 2). Figs. 2(a)-(c) also show that the numerical dispersion errors are slightly different in different propagation directions. The maximal difference of the numerical dispersion between different propagation directions is about 3.64%

(See Table 2). This implies that the eighth-order NAD-RK method has very small numerical dispersion and weak numerical dispersion anisotropy. From Fig. 2(a) we can find that the numerical phase-velocity for the eighth-order NAD-RK method is smaller than the exact phase-velocity. However, from Figs. 2(b)-(c) we can find that the numerical phase-velocity for the eighth-order NAD-RK method is greater than the exact phase-velocity. However, the overall variation of the numerical dispersion error for different Courant numbers and propagation directions is still less than 8% (See Table 1).

Figs. 2(d)-(f) and Figs. 2(g)-(i) show the numerical dispersion curves of the eighth-order LWC method and the eighth-order SG method, respectively. Compared with Figs. 2(a)-(c), the numerical dispersion shown in Figs. 2(d)-(i) is more serious. In Figs. 2(d)-(f), the maximum dispersion error of the eighth-order LWC method is about 18.77% (See Table 1) and the maximum dispersion error in Figs. 2(g)-(i) of the eighth-order SG method is about 17.88% (See Table 1), while the maximum dispersion errors of the eighth-order NAD-RK method in Figs. 2(a)-(c) are less than 8% (See Table 1). On the other

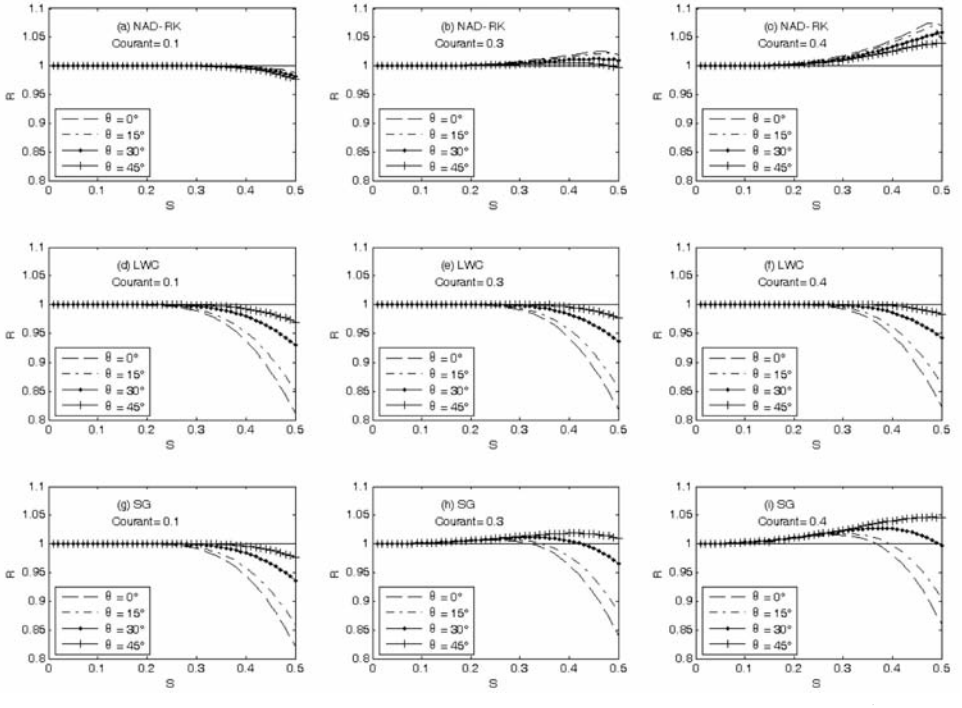

Fig. 2. The numerical dispersion ratio of the eighth-order NAD-RK method, the eighth-order LWC method, and the eighth-order SG method for the Courant numbers 0.1, 0.3, and 0.4, in four directions of $\theta = 0°$, 15°, 30°, and 45°.

hand, Figs. 2(d)-(f) and Figs. 2(g)-(i) show that there are large differences of the dispersion errors in different wave propagation directions for the eighth-order LWC and SG methods. From Table 2, The maximal difference of the maximal dispersion errors in different directions are about 15.94% for the eighth-order LWC and 18.58% for the eighth-order SG, respectively, while the maximal difference of the maximal dispersion errors of the eighth-order NAD-RK method in different directions is about 3.64% as mentioned earlier. In short, the eighth-order NAD-RK method has much less numerical dispersion than the eighth-order LWC and SG methods.

Table 1. The maximum dispersion errors in different wave propagation directions for different methods at different Courant numbers.

Method	The eighth-order NAD-RK method	The eighth-order LWC method	The eighth-order SG method
Courant = 0.1	0.023876	0.187670	0.178835
Courant = 0.3	0.025420	0.181909	0.15929
Courant = 0.4	0.074230	0.176561	0.139844

Table 2. The maximum differences of the maximum dispersion errors in different wave propagation directions for different methods at different Courant numbers.

Method	The eighth-order NAD-RK method	The eighth-order LWC method	The eighth-order SG method
Courant = 0.1	0.012352	0.157039	0.154933
Courant = 0.3	0.023550	0.158388	0.169269
Courant = 0.4	0.036430	0.159411	0.185804

Now we examine the numerical dispersion of the eighth-order NAD-RK method through the comparison of waveforms computed by different methods. We consider the 2D acoustic wave equation as follows

$$\partial^2 u/\partial t^2 = c_0^2[(\partial^2 u/\partial x^2) + (\partial^2 u/\partial z^2)] + f(t) \quad . \tag{13}$$

Here we choose the acoustic-wave propagating in a homogeneous medium with the acoustic velocity of 4 km/s. The time increment is $\Delta t = 0.005$ s and the recorded time length is $T = 1.2$ s. The receiver R is located at $(x,z) = (7$ km, 7 km). The model domain with a uniform grid spacing ($\Delta x = \Delta z = 50$ m) is $0 \leq x,z \leq 12$ km. The source with a frequency of $f_0 = 16$ Hz is located at the center of the model domain. The source function is chosen by

$$f(t) = \sin(2\pi f_0 t)\exp(-\pi^2 f_0^2 t^2/4) \quad . \tag{14}$$

In order to investigate the effect of the spatial increment on the numerical dispersion, we define the grid points per minimum wavelength (Dablain, 1986) as $G = v_{min}/(f_0 \cdot \Delta x)$. Here, v_{min} denotes the minimum acoustic wave-velocity and f_0 is the peak frequency.

Fig. 3 shows the waveforms recorded at receiver R on a coarse grid ($\Delta x = \Delta z = 50$ m), where the solid line denotes the exact solution calculated using the Cagniard-de Hoop technique (de Hoop, 1960) and the dashed lines denote the numerical solutions calculated by the eighth-order NAD-RK method [Fig. 3(a)], the eighth-order LWC method [Fig. 3(b)], and the eighth-order SG method [Fig. 3(c)], respectively. In this experiment, we have $G = 5$ for the case of $\Delta x = \Delta z = 50$ m in generating Fig. 3. Fig. 3(a) shows that the waveform computed by the eighth-order NAD-RK method is identical with the analytic solution for the coarse grid case ($\Delta x = \Delta z = 50$ m), whereas the high-order LWC and SG methods cause serious numerical dispersion [Figs. 3(b) and 3(c)] for the same grid size. This comparison demonstrates that the eighth-order NAD-RK method can provide the same accurate waveform as the analytic solution and can effectively eliminate the numerical dispersion caused by discretizing the wave equation for the coarse grid case. It also suggests that the eighth-order NAD-RK can increase computational efficiency and save computer memory if a coarse grid is used for large scale wavefield simulations.

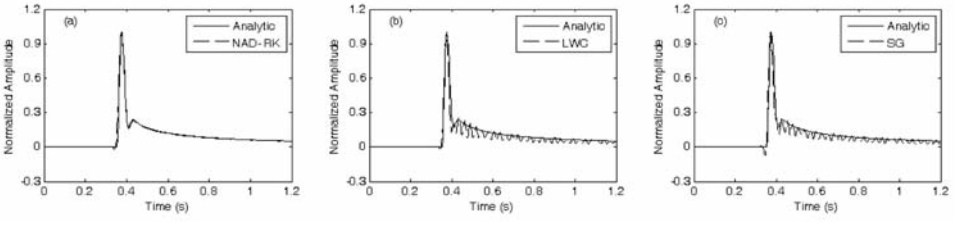

Fig. 3 Comparison of waveforms with the analytical solution for the homogenous medium, generated by (a) the eighth-order NAD-RK method, (b) the eighth-order LWC method, and (c) the eighth-order SG method, respectively.

COMPUTATIONAL EFFICIENCY

In this section, we examine the numerical dispersion and computational efficiency of the eighth-order NAD-RK method for the 2D case through the comparison of waveforms and wavefield snapshots computed by different methods.

Here, we choose the same equation as (13) with a velocity of $c_0 = 4$ km/s. The Courant number and the recorded time length are $\alpha = c_0\Delta t/\Delta x = 0.28$ and $T = 1.0$ s, respectively. The receiver R is located at (x,z) = (7 km, 7 km). The computational domain is $0 \leq x,z \leq 12$ km with the mesh spacing $\Delta x = \Delta z = 40$ m. The explosive source with a frequency of $f_0 = 40$ Hz is located at the center of the model domain. The source function is

$$f(t) = -5.76f_0^2[1 - 16(0.6f_0t - 1)^2] \times \exp[-8(0.6f_0t - 1)^2] \quad . \qquad (15)$$

Fig. 4 shows the wavefield snapshots on the coarse grid of $\Delta x = \Delta z = 40$ m at $T = 1.0$ s, generated by the eighth-order NAD-RK method [Fig. 4(a)], the eighth-order LWC scheme [Fig. 4(b)], and the eighth-order SG scheme [Fig. 4(c)], respectively. From Fig. 4, we can observe that the wavefronts of acoustic-waves, computed by three methods, are almost identical. However, the wavefield snapshot [Fig. 4(a)], generated by the eighth-order NAD-RK method on the coarse grid of $\Delta x = \Delta z = 40$ m, shows no visible numerical dispersion, whereas Figs. 4(b)-4(c), computed by the eighth-order LWC and SG methods on the same mesh, show serious numerical dispersion.

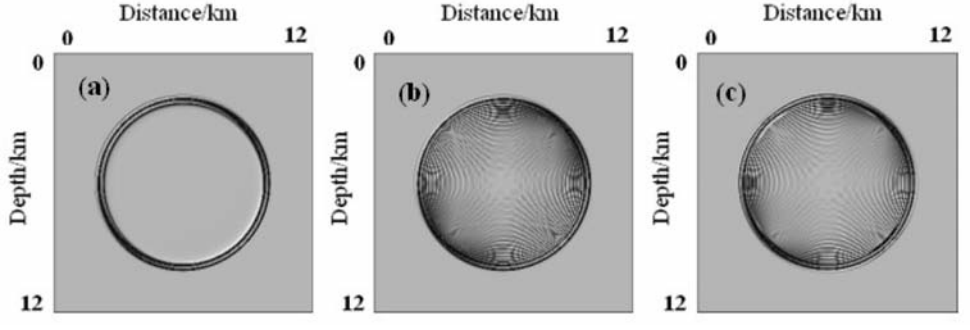

Fig. 4. The snapshots of acoustic wave fields at time $T = 1.0$ s on the coarse grid of $\Delta x = \Delta z = 40$ m, generated by (a) the eighth-order NAD-RK method, (b) the eighth-order LWC method, and (c) the eighth-order SG method, respectively.

Fig. 5 shows the waveforms recorded at receiver R on a coarse grid of $\Delta x = \Delta z = 40$ m, calculated by the eighth-order NAD-RK method [Fig. 5(a)],

the eighth-order LWC scheme [Fig. 5(b)], the eighth-order SG scheme [Fig. 5(c)], respectively. Fig. 5(a) shows that the waveform computed by the eighth-order NAD-RK method has no numerical dispersion for the coarse grid case of $\Delta x = \Delta z = 40$ m, whereas the eighth-order LWC and SG methods cause serious numerical dispersion [Figs. 5(b) and 5(c)] for the same grid size. This comparison shows that the eighth-order NAD-RK method can provide a highly accurate waveform and can effectively eliminate the numerical dispersion caused by discretizing the wave equation for the coarse grid case. It implies that the eighth-order NAD-RK method can increase computational efficiency and save computer memory when a coarse grid is used for large scale wavefield simulations.

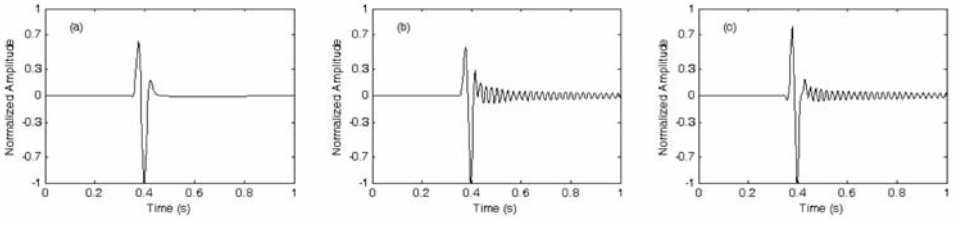

Fig. 5. The waveforms at the receiver R(7km,7km) on the coarse grid of $\Delta x = \Delta z = 40$ m, generated by (a) the eighth-order NAD-RK method, (b) the eighth-order LWC method, and (c) the eighth-order SG method, respectively.

To further test the computational efficiency of the eighth-order NAD-RK method, next we show wavefield snapshots calculated by the eighth-order LWC method and the eighth-order SG method on fine grids. To exactly eliminate the numerical dispersion, the space grids are chosen as $\Delta x = \Delta z = 18$ m for the eighth-order LWC method and $\Delta x = \Delta z = 20$ m for the eighth-order SG method, corresponding to the numbers of grid points of 668×668 and 601×601, respectively. While for the same computational domain, the number of mesh points for the eighth-order NAD-RK method is only 301×301 on the coarse grid of $\Delta x = \Delta z = 40$ m. Here, we have $G = 2.5$ for generating Fig. 4(a), $G = 5.6$ for generating Fig. 6(a) and $G = 5$ for generating Fig. 6(b). As a result, the memory requirement of the eighth-order NAD-RK method is approximately 20% of that of the eighth-order LWC method and approximately 25% of that of the eighth-order SG scheme.

Fig. 6 shows the wavefield snapshots on the fine grid, generated by the eighth-order LWC method ($\Delta x = \Delta z = 18$ m) and the eighth-order SG method ($\Delta x = \Delta z = 20$ m) for the same Courant number as that in the coarse mesh of 40 m. The comparison between Fig. 4(a) and Fig. 6 demonstrates that the

eighth-order NAD-RK method on a coarse grid ($\Delta x = \Delta z = 40$ m) can provide the same numerical accuracy as those of the eighth-order LWC and SG methods on fine grids. But the computational cost of the eighth-order NAD-RK method is completely different from those of the eighth-order LWC and SG schemes. For instance, to generate Fig. 4(a), it takes the eighth-order NAD-RK method about 56 s, whereas to generate Figs. 6(a)-(b) it takes the eighth-order LWC method and the eighth-order SG method about 325 s and 85 s, respectively. This demonstrates that the computational speed of the eighth-order NAD-RK method is roughly 5.8 times of the eighth-order LWC method and about 1.52 times of the eighth-order SG method to achieve the same accuracy. All our examples are computed on a 2-core Pentium 4 computer with 2.33G memory.

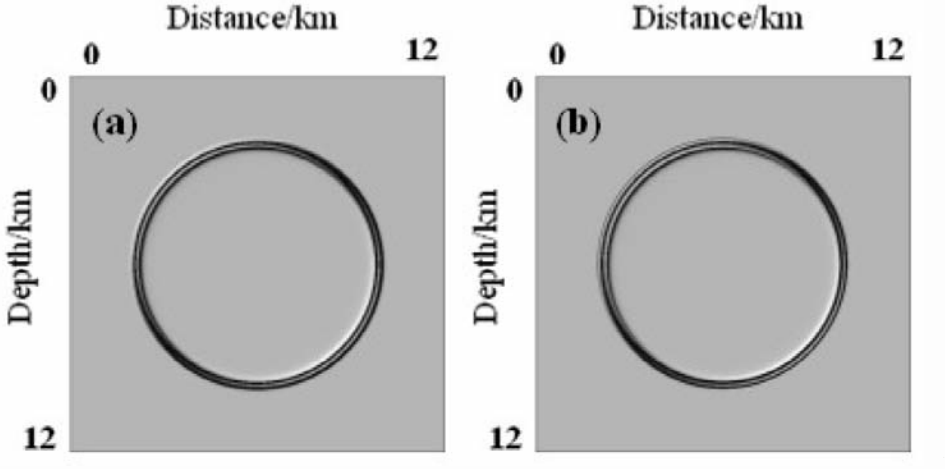

Fig. 6. Snapshots of wave-fields at time T = 1.0 s on the fine grids, generated by (a) the eighth-order LWC method ($\Delta x = \Delta z = 18$ m) and (b) the eighth-order SG method ($\Delta x = \Delta z = 20$ m).

NUMERICAL SIMULATIONS

In this section we will show some numerical examples to demonstrate the performance of the eighth-order NAD-RK method in suppressing the numerical dispersion through choosing two 2D acoustic models and comparing the numerical results computed by the eighth-order NAD-RK method, the eighth-order LWC, SG, and TSD-FD methods.

Two-layer acoustic model

In the first example, we choose a two-layer acoustic model with the velocities in the upper and lower layers being 2.4 km/s and 5.0 km/s. The

computational domain is $0 \leq x \leq 25$ km and $0 \leq z \leq 25$ km. The horizontal interface is at a depth of 15 km. The explosive source of eq. (15) with $f_0 = 16$ Hz is at coordinate (12.5 km, 14 km). The receiver R is located at (13.3 km, 12.9 km). The spatial increment and time step are $h = \Delta x = \Delta z = 50$ m and $\Delta t = 0.002$ s, resulting in $G = 3$.

The wavefield snapshots and waveforms, computed by the eighth-order NAD-RK method, the eighth-order LWC method, the eighth-order SG method, and the eighth-order TSD-FD method, are shown in Figs. 7 and 8. Figs. 7(a) and 8(a), generated by the eighth-order NAD-RK method, show clear wavefield snapshots and waveforms, and almost no visible numerical dispersion although such coarse grids of $\Delta x = \Delta z = 50$ m are used. However, from Figs. 7(b-d) and 8(b-d), we can see that the eighth-order LWC method [Figs. 7(b) and 8(b)], the eighth-order SG method [Figs. 7(c) and 8(c)], and the eighth-order TSD-FD method [Figs. 7(d) and 8(d)] suffer from serious numerical dispersions. This numerical experiment demonstrates that the eighth-order NAD-RK method can provide high accuracy for the layered medium with strong discontinuities.

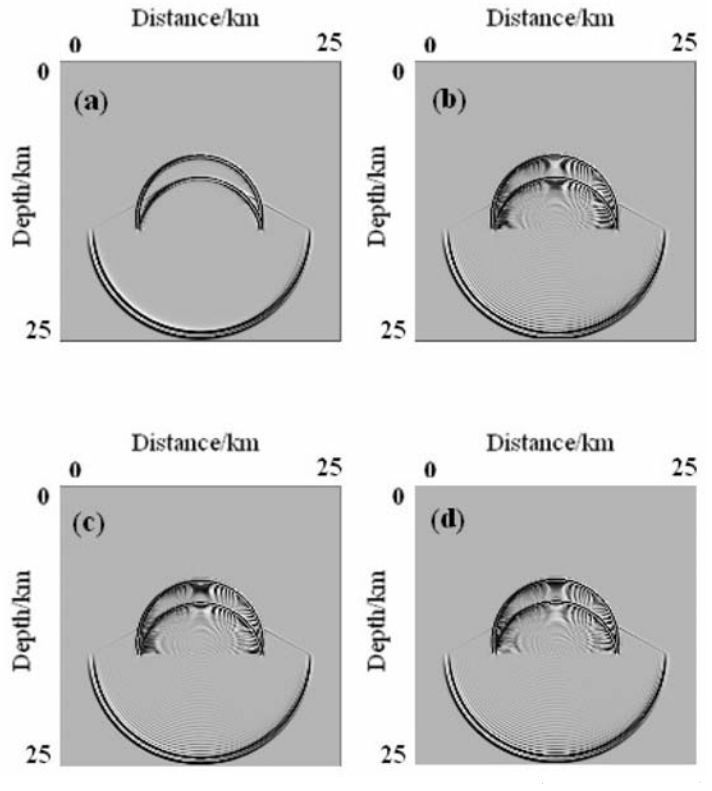

Fig. 7. Snapshots of wave fields at time $T = 2.4$ s on the coarse grid of $\Delta x = \Delta z = 50$ m for the two-layer model, generated by (a) the eighth-order NAD-RK method, (b) the eighth-order LWC method, (c) the eighth-order SG method, and (d) the eighth-order TSD-FD method, respectively.

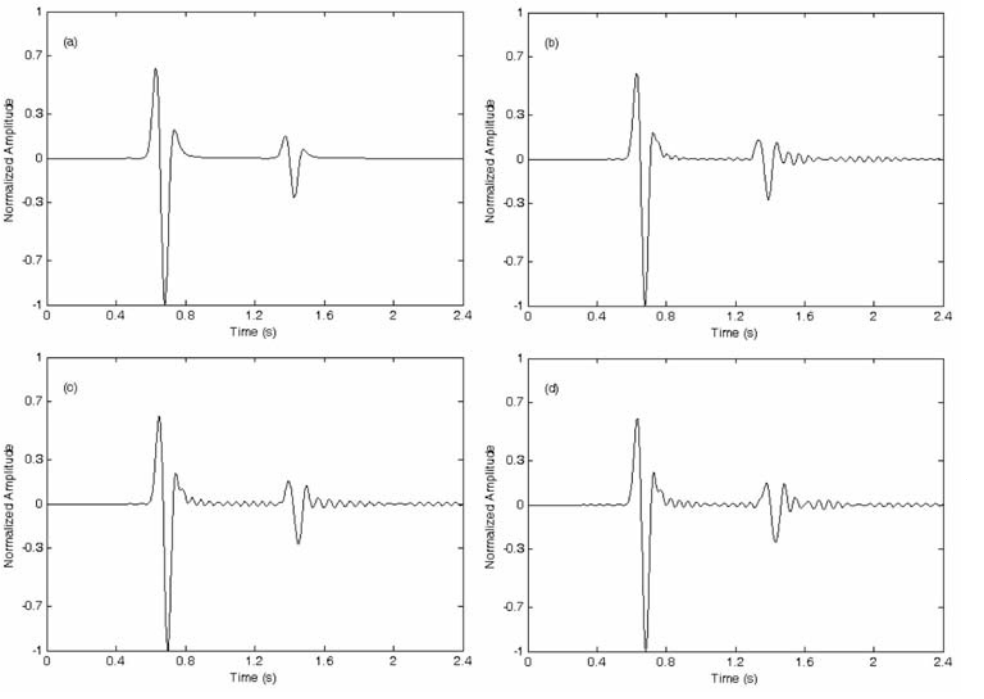

Fig. 8. The waveforms at the receiver R (13.3km, 12.9km) on the coarse grid of $\Delta x = \Delta z = 50$ m, generated by (a) the eighth-order NAD-RK method, (b) the eighth-order LWC method, (c) the eighth-order SG method, and (d) the eighth-order TSD-FD method, respectively.

Heterogeneous acoustic model

In the last experiment, we investigate the effectiveness of the eighth-order NAD-RK method, the eighth-order LWC method, the eighth-order SG method, and the eighth-order TSD-FD method for the heterogeneous acoustic case. We choose a three-layer model, and velocity of every layer is shown in Fig. 9. Here, the spatial increment and time step are chosen as $\Delta x = \Delta z = 40$ m and $\Delta t = 2.0$ ms. The source, located at the center of the computational domain, is a Ricker wavelet with frequency $f_0 = 20$ Hz [see eq. (15)], where $G = 3$.

The wavefield snapshots at 1.4 s are shown in Figs. 10(a)-(d), generated by the eighth-order NAD-RK method, the eighth-order LWC method, the eighth-order SG method, and the eighth-order TSD-FD method, respectively. From Fig. 10(a), we can see that the eighth-order NAD-RK method has no numerical dispersion, whereas Figs. 10(b)-(d) show that the eighth-order LWC, SG and TSD-FD methods cause serious numerical dispersion.

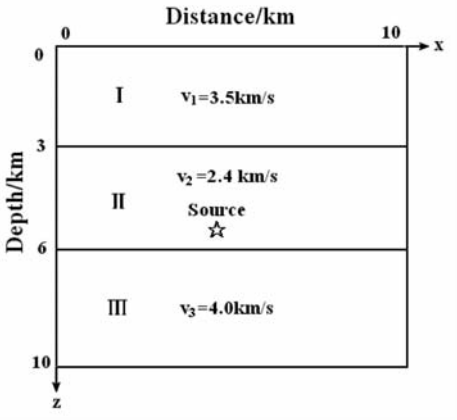

Fig. 9. A three-layer heterogeneous acoustic model.

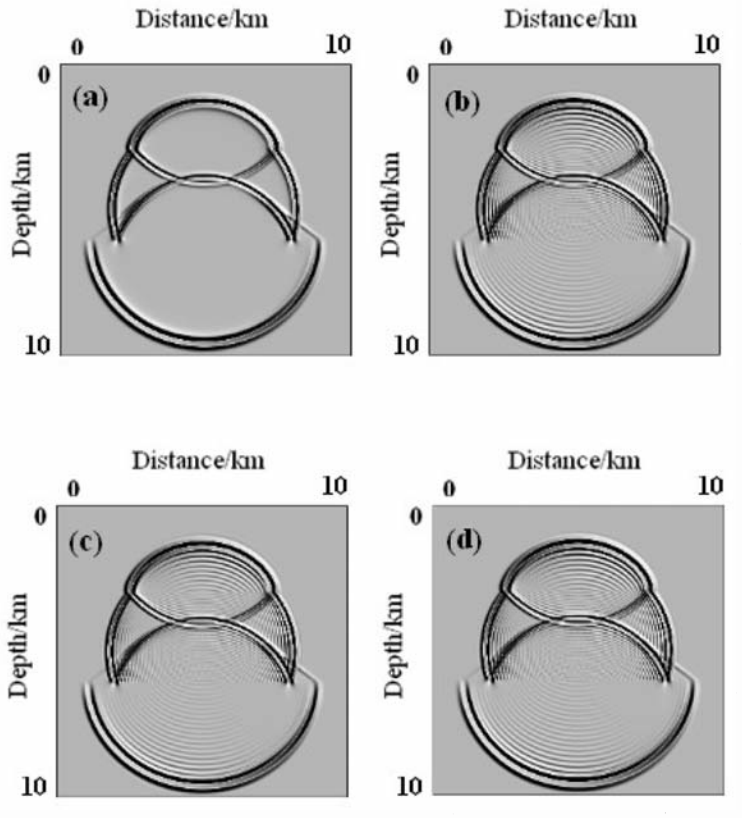

Fig. 10. Snapshots of wave fields at time T = 1.4 s on the coarse grid of $\Delta x = \Delta z = 40$ m for the three-layer model, generated by (a) the eighth-order NAD-RK method, (b) the eighth-order LWC method, (c) the eighth-order SG method, and (d) the eighth-order TSD-FD method, respectively.

DISCUSSION AND CONCLUSIONS

In this paper, we have proposed a new numerical method to solve the 2D acoustic wave equation, which is called the eighth-order NAD-RK method. The method uses the high-order NAD operators to approximate the high-order spatial differential operator and applies the third-order Runge-Kutta method to perform the time discretization. As a result, the eighth-order NAD-RK method has third-order accuracy in time and eighth-order accuracy in space.

First, we transform the 2D acoustic wave equations into the ODEs (5) or (6) and give the computational formulae (2) or (3) of the third-order RK method for temporal discretization to solve the converted ODEs. Then we use the computational formulae of the eighth-order nearly-analytic discretizations (see Appedix A) to approximate the second- and third-order spatial derivatives, which are included in the converted ODEs. Meanwhile, following the Fourier analysis, we obtain the stability condition for the 2D case through a series of mathematical operations (see Appedix B). The numerical error of the eighth-order NAD-RK method is much smaller than those of the same order schemes such as the eighth-order LWC and the eighth-order SG methods, which is confirmed by the relative errors shown in Fig. 1. Then, after detailed derivations (see Appendix C), we get the dispersion relations (C-2) and (C-3) of the eighth-order NAD-RK method, and compare the numerical dispersions ratios and the waveforms of the eighth-order NAD-RK method against the eighth-order LWC and SG methods. The results show that the eighth-order NAD-RK method has the smallest numerical dispersion among the three methods. In other words, the eighth-order NAD-RK method can effectively suppress the numerical dispersion.

By analyzing computational efficiency of the eighth-order NAD-RK method from the waveforms and wavefield snapshots computed by the eighth-order NAD-RK method, the eighth-order LWC method, and the eighth-order SG method, we conclude that the eighth-order method requires less computer memory and has higher computational speed to achieve the same computational accuracy when a coarse mesh is used for large scale wavefield simulations. At last, we choose two 2D acoustic layered models with large velocity contrasts to demonstrate the performance of the eighth-order NAD-RK method in suppressing the numerical dispersion, and compare those numerical results computed by the eighth-order NAD-RK method, the eighth-order LWC method, the eighth-order SG method, and the eighth-order TSD-FD method. These results further illustrate that the eighth-order NAD-RK method has a very good effect in suppressing the numerical dispersion and can provide high accuracy for the layered model with strong discontinuities. Therefore, we conclude that the eighth-order NAD-RK method has potential applications in large-scale wave fields modeling, seismic tomography and inversion.

ACKNOWLEDGEMENTS

This work was supported by the National Natural Science Foundation of China (Grant No.41230210), and the Science Foundation of the Education Department of Yunnan Province (No.2013Z152). Meanwhile, this work was also supported partly by Statoil Company (Contract No.4502502663).

REFERENCES

Blanch, J.O. and Robertsson, A., 1997. A modified Lax-Wendroff correction for wave propagation in media described by Zener elements. Geophys. J. Internat., 131: 381-386.

Chen, J.B., 2007. High-order time discretizations in seismic modeling. Geophysics, 72: 115-122.

Chen, K.H., 1984. Propagating numerical model of elastic wave in anisotropic in homogeneous media-finite element method. Expanded Abstr., 54th Ann. Internat. SEG Mtg., Atlanta: 631-632.

Chen, S., Yang, D.H. and Deng, X.Y., 2010. An improved algorithm of the fourth-order Runge-Kutta method and seismic wave-field simulation. Chin. J. Geophys. (in Chinese), 53: 1196-1206.

Chen, X.F., 1993. A systematic and efficient method of computing normal modes for multi-layered half space. Geophys. J. Internat., 115: 391-409.

Dablain, M.A., 1986. The application of high-order differencing to scalar wave equation. Geophysics, 51: 54-66.

de Hoop, A.T., 1960. A modification of Cagniard's method for solving seismic pulse problems. Appl. Sci. Res., B8: 349-356.

Dong, L.G., Ma, Z.T., Cao, J.Z., Wang, H.Z., Geng, J.H., Lei, B. and Xu, S.Y., 2000. A staggered-grid high-order difference method of one-order elastic wave equation. Chin. J. Geophys. (in Chinese), 43: 411-419.

Finkelstein, B. and Kästner, R., 2007. Finite difference time domain dispersion reduction schemes. J. Comput. Phys, 221: 422-438.

Finkelstein, B. and Kästner, R., 2008. A comprehensive new methodology for formulating FDTD schemes with controlled order of accuracy and dispersion. IEEE, Trans. Antenna Propagat, 56: 3516-3525.

Huang, B.S., 1992. A program for two-dimensional seismic wave propagation by the pseudo-spectrum method. Comput. Geosci., 18: 289-307.

Kelly, K.R. and Marfurt, K.J. (Eds.), 1990. Numerical Modeling of Seismic Wave Propagation. Geophys. Repr. Ser., 13.

Kelly, K.R. and Wave, R.W., 1976. Synthetic seismograms: a finite-difference approach. Geophysics, 41: 2-27.

Komatitsch, D. and Vilotte, J.P., 1998. The spectral element method: an efficient tool to simulate the seismic responses of 2D and 3D geological structures. Bull. Seismol. Soc. Am., 88: 368-392.

Kosloff, D. and Baysal, E., 1982. Forward modeling by the Fourier method. Geophysics, 47: 1402-1412.

Kosloff, D., Reshef, M. and Loewenthal, D., 1984. Elastic wave calculations by the Fourier method. Bull. Seismol. Soc. Am., 74: 875-891.

Lax, P.D. and Wendroff, B., 1964. Difference schemes for hyperbolic equations with high order of accuracy. Communic. Pure Appl. Mathemat., 17: 381-398.

Lele, S.K., 1992. Compact finite difference schemes with spectral-like resolution. J. Comput. Phys., 103: 16-42.

Liu, Y. and Sen, M.K., 2009. A new time-space domain high-order finite-difference method for the acoustic wave equation. J. Comput. Phys., 228: 8779-8806.

Marfurt, K.J., 1984. Accuracy of finite-difference and finite-element modeling of the scalar and elastic wave equations. Geophysics, 49: 533-549.

Ma, S. and Liu, P., 2006. Modeling of the perfectly matched layer absorbing boundaries and intrinsic attenuation in explicit finite-element methods. Bull. Seismol. Soc. Am., 96: 1779-1794.

Moczo, P., Kristek, J. and Halada, L., 2000. 3D 4th-order staggered-grid finite-difference schemes: stability and grid dispersion. Bull. Seismol. Soc. Am, 90: 587-603.

Moczo, P., Kristek, J., Galis, M., Pazak, P. and Balazovjech, M., 2007. The finite-difference and finite-element modeling of seismic wave propagation and earthquake motion. Acta Phys. Slovaca, 57: 177-406.

Moczo, P., Kristek, J., Vavryčuk, V., Archuleta, R.J. and Halada, L., 2002. 3D heterogeneous staggered-grid finite-difference modeling of seismic motion with volume harmonic and arithmetic averaging of elastic moduli and densities. Bull. Seismol. Soc. Am., 92: 3042-3066.

Qiu, J.X., Li, T.G. and Khoo, B.C., 2008. Simulations of compressible two-medium flow by Runge-Kutta discontinuous Galerkin methods with the ghost fluid method. Communic. Comput. Phys., 3: 479-504.

Saenger, E.H., Gold, N. and Shapiro, S.A., 2000. Modeling the propagation of elastic waves using a modified finite-difference grid. Wave Motion, 31: 77-92.

Seriani, G. and Priolo, E., 1994. Spectral element method for acoustic wave simulation in heterogeneous media. Finite Elem. Analysis Design, 16: 337-348.

Smith, W.D., 1975. The application of finite element analysis to body wave propagation problems. Geophys. J., 42: 747-768.

Tong, P., Yang, D.H., Hua, B.L. and Wang, M.X., 2013. An high-order stereo-modeling method for solving wave equations. Bull. Seismol. Soc. Am., 103: 811-833.

Virieux, J., 1986. P-SV wave propagation in heterogeneous median: Velocity-stress finite-difference method. Geophysics, 51: 889-901.

Wang, L., Yang, D.H. and Deng, X.Y., 2009. A WNAD method for seismic stress-field modeling in heterogeneous media. Chin. J. Geophys. (in Chinese), 52: 1526-1535.

Yang, D.H., 2002. Finite element method of the elastic wave equation and wave field simulation in two-phase anisotropic media. Chin. J. Geophys. (in Chinese), 45: 575-583.

Yang, D.H., Liu, E., Zhang, Z.J. and Teng, J.W., 2002. Finite-difference modeling in two-dimensional anisotropic media using a flux-corrected transport technique. Geophys. J. Internat., 148: 320-328.

Yang, D.H., Peng, J.M., Lu, M. and Terlaky, T., 2006. Optimal nearly-analytic discrete approximation to the scalar wave equation. Bull. Seismol. Soc. Am., 96: 1114-1130.

Yang, D.H., Song, G.J. and Lu, M., 2007. Optimally accurate nearly analytic discrete for wave-field simulation in 3D anisotropic media. Bull. Seismol. Soc. Am., 97, 1557-1569.

Yang, D.H., Song, G.J., Chen, S. and Hou, B.Y., 2007. An improved nearly analytical discrete method: an efficient tool to simulate the seismic response of 2-D porous structures. J. Geophys. Engin., 4: 40-52.

Yang, D.H., Teng, J.W., Zhang, Z.J. and Liu, E., 2003. A nearly-analytic discrete method for acoustic and elastic wave equations in anisotropic media. Bull. Seismol. Soc. Am., 93: 882-890.

Yang, D.H., Tong, P. and Deng, X.Y., 2012. A central difference method with low numerical dispersion for solving the scalar wave equation. Geophys. Prosp., 60, 885-905.

Yang, D.H., Wang, L. and Deng, X.Y., 2010. An explicit split-step algorithm of the implicit Adams method for solving 2D acoustic and elastic wave equations. Geophys. J. Internat., 180: 291-310.

Yang, D.H., Wang, N., Chen, S. and Song, G.J., 2009. An explicit method based on the implicit Runge-Kutta algorithm for solving the wave equations. Bull. Seismol. Soc. Am., 99: 3340-3354.

Zeng, Y.Q. and Liu, Q.H., 2001. A staggered-grid finite-difference method with perfectly matched layers for poroelastic wave equations. J. Acoust. Soc. Am., 109: 2571-2580.

Zhang, Z.J., Wang, G.J. and Harris, J.M., 1999. Multi-component wave-field simulation in viscous extensively dilatancy anisotropic media. Phys. Earth Planet. Inter., 114: 25-38.

Zheng, H.S., Zhang, Z.J. and Liu, E., 2006. Non-linear seismic wave propagation in anisotropic media using the flux-corrected transport technique. Geophys. J. Internat., 165: 943-956.

APPENDIX A

APPROXIMATION OF HIGH-ORDER DERIVATIVES

In order to obtain the approximation formulae of high-order derivatives in eq. (6) for the 2D case, Tong et al. (2013) derived these approximate formulae. For convenience, here we present the approximation formulae of the displacement **u** as follows

$$\partial^2\mathbf{u}_{j,k}/\partial x^2 = (1/\Delta x^2)[(7/54)(\mathbf{u}_{j-2,k}+\mathbf{u}_{j+2,k}) + (64/27)(\mathbf{u}_{j-1,k}+\mathbf{u}_{j+1,k}) - 5\mathbf{u}_{j,k}]$$
$$+ (1/\Delta x)[(1/36)\{(\partial\mathbf{u}_{j-2,k}/\partial x)-(\partial\mathbf{u}_{j+2,k}/\partial x)\} + (8/9)\{(\partial\mathbf{u}_{j-1,k}/\partial x)-(\partial\mathbf{u}_{j+1,k}/\partial x)\}] \quad , \quad \text{(A-1)}$$

$$\partial^2\mathbf{u}_{j,k}/\partial z^2 = (1/\Delta z^2)[(7/54)(\mathbf{u}_{j,k-2}+\mathbf{u}_{j,k+2}) + (64/27)(\mathbf{u}_{j,k-1}+\mathbf{u}_{j,k+1}) - 5\mathbf{u}_{j,k}]$$
$$+ (1/\Delta z)[(1/36)\{(\partial\mathbf{u}_{j,k-2}/\partial z)-(\partial\mathbf{u}_{j,k+2}/\partial z)\} + (8/9)\{(\partial\mathbf{u}_{j,k-1}/\partial z)-(\partial\mathbf{u}_{j,k+1}/\partial z)\}] \quad , \quad \text{(A-2)}$$

$$\partial^3\mathbf{u}_{j,k}/\partial x^3 = (1/\Delta x^3)[-(31/144)(\mathbf{u}_{j-2,k}-\mathbf{u}_{j+2,k}) - (88/9)(\mathbf{u}_{j-1,k}-\mathbf{u}_{j+1,k})]$$
$$+ (1/\Delta x^2)[-(1/24)\{(\partial\mathbf{u}_{j-2,k}/\partial x)+(\partial\mathbf{u}_{j+2,k}/\partial x)\}$$
$$- (8/3)\{(\partial\mathbf{u}_{j-1,k}/\partial x)+(\partial\mathbf{u}_{j+1,k}/\partial x)\} - 15\partial\mathbf{u}_{j,k}/\partial x] \quad , \quad \text{(A-3)}$$

$$\partial^3\mathbf{u}_{j,k}/\partial z^3 = (1/\Delta x^3)[-(31/144)(\mathbf{u}_{j,k-2}-\mathbf{u}_{j,k+2}) - (88/9)(\mathbf{u}_{j,k-1}-\mathbf{u}_{j,k+1})]$$
$$+ (1/\Delta z^2)[-(1/24)\{(\partial\mathbf{u}_{j,k-2}/\partial z)+(\partial\mathbf{u}_{j,k+2}/\partial z)\}$$
$$- (8/3)\{(\partial\mathbf{u}_{j,k-1}/\partial z)+(\partial\mathbf{u}_{j,k+1}/\partial z)\} - 15\partial\mathbf{u}_{j,k}/\partial z] \quad , \quad \text{(A-4)}$$

$$\partial^3\mathbf{u}_{j,k}/\partial x\partial z^2 = (31/864\Delta x\Delta z^2)(\mathbf{u}_{j+2,k+2} - \mathbf{u}_{j-2,k-2} + \mathbf{u}_{j+2,k-2} - \mathbf{u}_{j-2,k+2} + 2\mathbf{u}_{j-2,k} - 2\mathbf{u}_{j+2,k})$$
$$+ (44/27\Delta x\Delta z^2)(\mathbf{u}_{j+1,k+1} - \mathbf{u}_{j-1,k-1} + \mathbf{u}_{j+1,k-1} - \mathbf{u}_{j-1,k+1} + 2\mathbf{u}_{j-1,k} - 2\mathbf{u}_{j+1,k})$$
$$- (1/144\Delta z^2)[(\partial\mathbf{u}_{j-2,k-2}/\partial x) + (\partial\mathbf{u}_{j+2,k+2}/\partial x) + (\partial\mathbf{u}_{j-2,k+2}/\partial x)$$
$$+ (\partial\mathbf{u}_{j+2,k-2}/\partial x) - 2\partial\mathbf{u}_{j+2,k}/\partial x - 2\partial\mathbf{u}_{j-2,k}/\partial x]$$
$$- (4/9\Delta z^2)[(\partial\mathbf{u}_{j-1,k-1}/\partial x) + (\partial\mathbf{u}_{j+1,k+1}/\partial x) + (\partial\mathbf{u}_{j-1,k+1}/\partial x)$$
$$+ (\partial\mathbf{u}_{j+1,k-1}/\partial x) - 2\partial\mathbf{u}_{j+1,k}/\partial x - 2\partial\mathbf{u}_{j-1,k}/\partial x]$$

$$- (1/144\Delta x\Delta z)[(\partial \mathbf{u}_{j-2,k-2}/\partial z) + (\partial \mathbf{u}_{j+2,k+2}/\partial z) - (\partial \mathbf{u}_{j-2,k+2}/\partial z) - (\partial \mathbf{u}_{j+2,k-2}/\partial z)]$$

$$- (4/9\Delta x\Delta z)[(\partial \mathbf{u}_{j-1,k-1}/\partial z) + (\partial \mathbf{u}_{j+1,k+1}/\partial z) - (\partial \mathbf{u}_{j-1,k+1}/\partial z) - (\partial \mathbf{u}_{j+1,k-1}/\partial z)] \quad , \tag{A-5}$$

$$\partial^3 \mathbf{u}_{j,k}/\partial x^2\partial z = (31/864\Delta x^2\Delta z)(\mathbf{u}_{j+2,k+2} - \mathbf{u}_{j-2,k-2} + \mathbf{u}_{j-2,k+2} - \mathbf{u}_{j+2,k-2} + 2\mathbf{u}_{j,k-2} - 2\mathbf{u}_{j,k+2})$$

$$+ (44/27\Delta x^2\Delta z)(\mathbf{u}_{j+1,k+1} - \mathbf{u}_{j-1,k-1} + \mathbf{u}_{j-1,k+1} - \mathbf{u}_{j+1,k-1} + 2\mathbf{u}_{j,k-1} - 2\mathbf{u}_{j,k+1})$$

$$- (1/144\Delta x^2)[(\partial \mathbf{u}_{j-2,k-2}/\partial z) + (\partial \mathbf{u}_{j+2,k+2}/\partial z) + (\partial \mathbf{u}_{j-2,k+2}/\partial z) + (\partial \mathbf{u}_{j+2,k-2}/\partial z) - 2\partial \mathbf{u}_{j,k+2}/\partial z - 2\partial \mathbf{u}_{j,k-2}/\partial z]$$

$$- (4/9\Delta x^2)[(\partial \mathbf{u}_{j-1,k-1}/\partial z) + (\partial \mathbf{u}_{j+1,k+1}/\partial z) + (\partial \mathbf{u}_{j-1,k+1}/\partial z) + (\partial \mathbf{u}_{j+1,k-1}/\partial z) - 2\partial \mathbf{u}_{j,k+1}/\partial z - 2\partial \mathbf{u}_{j,k-1}/\partial z]$$

$$- (1/144\Delta x\Delta z)[(\partial \mathbf{u}_{j-2,k-2}/\partial x) + (\partial \mathbf{u}_{j+2,k+2}/\partial x) - (\partial \mathbf{u}_{j-2,k+2}/\partial x) - (\partial \mathbf{u}_{j+2,k-2}/\partial x)]$$

$$- (4/9\Delta x\Delta z)[(\partial \mathbf{u}_{j-1,k-1}/\partial x) + (\partial \mathbf{u}_{j+1,k+1}/\partial x) - (\partial \mathbf{u}_{j-1,k+1}/\partial x) - (\partial \mathbf{u}_{j+1,k-1}/\partial x)] \quad , \tag{A-6}$$

where Δx, Δz denote the space increment in the x- and z-directions, respectively.

Similarly, the corresponding computational formulae related to the particle-velocity w can be obtained simply by substituting **u** by **w** into (A-1)-(A-6).

APPENDIX B

DERIVATION OF STABILITY CRITERION

To obtain the stability condition of the eighth-order NAD-RK method for the 2D case, for simplicity we consider the harmonic solution of eq. (7) under the condition $\Delta x = \Delta z = h$. Substituting the solution

$$U^n_{j,l} = U^n \exp[i\bar{k}(j\Delta x\cos\theta + l\Delta z\sin\theta)] \quad , \tag{B-1}$$

where

$$U^n_{j,l} = [\mathbf{u}^n_{j,l},\ (\partial\mathbf{u}/\partial x)^n_{j,l},\ (\partial\mathbf{u}/\partial z)^n_{j,l},\ \mathbf{v}^n_{j,l},\ (\partial\mathbf{v}/\partial x)^n_{j,l},\ (\partial\mathbf{u}/\partial z)^n_{j,l}] \ ,$$

$$U^n = [\mathbf{u}^n,\ (\partial\mathbf{u}^n/\partial x),\ (\partial\mathbf{u}^n/\partial z),\ \mathbf{v}^n,\ (\partial\mathbf{v}^n/\partial x),\ (\partial\mathbf{v}^n/\partial z)] \ ,$$

into eq. (7) with relations (A-1) to (A-6), we can obtain the following equation

$$[\mathbf{u}^{n+1},(\partial\mathbf{u}^{n+1}/\partial x),(\partial\mathbf{u}^{n+1}/\partial z),\mathbf{v}^{n+1},(\partial\mathbf{v}^{n+1}/\partial x),(\partial\mathbf{v}^{n+1}/\partial z)]^T$$

$$= \mathbf{G}[\mathbf{u}^n,(\partial\mathbf{u}^n/\partial x),(\partial\mathbf{u}^n/\partial z),\mathbf{v}^n,(\partial\mathbf{v}^n/\partial x),(\partial\mathbf{v}^n/\partial z)]^T \ . \qquad \text{(B-2)}$$

Due to the complexity of the elements g_{ij} of the amplification matrix **G**, here we only show the first and second row of **G** as follows

$$g_{11} = 1 + [-5 + (64/27)\cos\xi + (7/54)\cos 2\xi + (64/27)\cos\eta + (7/54)\cos 2\eta]\alpha^2 \ ,$$

$$g_{12} = -[(8/9)\sin\xi + (1/36)\sin 2\xi]ih\alpha^2 \ ,$$

$$g_{13} = -[(8/9)\sin\eta + (1/36)\sin 2\eta]ih\alpha^2 \ ,$$

$$g_{14} = t + [-(5/3) + (64/81)\cos\xi + (7/162)\cos 2\xi + (64/81)\cos\eta + (7/162)\cos 2\eta]t\alpha^2$$

$$g_{15} = -[(8/27)\sin\xi + (1/108)\sin 2\xi]iht\alpha^2 \ ,$$

$$g_{16} = -[(8/27)\sin\eta + (1/108)\sin 2\eta]iht\alpha^2 \ ,$$

$$g_{21} = [(176/27)\sin\xi + (31/216)\sin 2\xi + (31/864)\sin(2\xi-2\eta) + (44/27)\sin(\xi-\eta)$$
$$+ (44/27)\sin(\xi+\eta) + (31/864)\sin(2\xi+2\eta)]i\alpha^2/h \ ,$$

$$g_{22} = 1 - [(15/2) + (16/9)\cos\xi + (1/36)\cos 2\xi + (1/144)\cos(2\xi-2\eta)$$
$$+ (4/9)\cos(\xi-\eta) + (4/9)\cos(\xi+\eta) + (1/144)\cos(2\xi+2\eta)]\alpha^2 \ ,$$

$$g_{23} = [(1/144)\cos(2\xi-2\eta) + (4/9)\cos(\xi-\eta) - (4/9)\cos(\xi+\eta)$$
$$- (1/144)\cos(2\xi+2\eta)]\alpha^2 \ ,$$

$$g_{24} = [-(31/2592)\sin(2\xi-2\eta) - (44/81)\sin(\xi-\eta) + (176/81)\sin\eta$$
$$+ (31/648)\sin 2\eta + (44/81)\sin(\xi+\eta) + (31/2592)\sin(2\xi+2\eta)]it\alpha^2/h \ ,$$

$$g_{25} = t + [(1/432)\cos(2\xi-2\eta) + (4/27)\cos(\xi-\eta) - (4/27)\cos(\xi+\eta)$$
$$- (1/432)\cos(2\xi+2\eta)]t\alpha^2 \ ,$$

$$g_{26} = -[(15/2) + (1/432)\cos(2\xi-2\eta) + (4/27)\cos(\xi-\eta) + (16/27)\cos\eta$$
$$+ (1/108)\cos 2\eta + (4/27)\cos(\xi+\eta) + (1/432)\cos(2\xi+2\eta)]t\alpha^2 \ ,$$

where $\Delta x = \Delta z = h$, $\xi = \bar{k}h\cos\theta$, $\eta = \bar{k}h\sin\theta$, $\alpha = c_0\Delta t/h$, $i = \sqrt{-1}$. $\bar{k}\cos\theta$ and $\bar{k}\sin\theta$ are the wave number, θ is the wave propagation angle with respect to the x-axis.

From the amplification matrix **G**, we can numerically obtain the following stability criterion of the eighth-order NAD-RK method for the 2D case by solving the eigenvalue problem $|\lambda_l(\mathbf{G})| \leq 1$ for all eigenvalues $\lambda_l(\mathbf{G})$, $l = 1,2,\ldots,6$.

$$\alpha \leq \alpha_{max} \approx 0.5416 \quad . \tag{B-3}$$

where α_{max} denotes the maximum Courant number.

APPENDIX C

DERIVATION OF THE NUMERICAL DISPERSION RELATION

To obtain the numerical dispersion relation of the eighth-order NAD-RK method for the 2D case, we consider the harmonic solution of eq. (7) while $\Delta x = \Delta z = h$ and substitute the solution

$$U^n_{j,l} = U^0\exp[i\{\omega_{num}n\Delta t + j(\bar{k}h\cos\theta) + l(\bar{k}h\sin\theta)\}] \quad , \tag{C-1}$$

where

$$U^n_{j,l} = [\mathbf{u}^n_{j,l}, (\partial\mathbf{u}/\partial x)^n_{j,l}, (\partial\mathbf{u}/\partial z)^n_{j,l}, \mathbf{v}^n_{j,l}, (\partial\mathbf{v}/\partial x)^n_{j,l}, (\partial\mathbf{v}/\partial z)^n_{j,l}] \quad ,$$

$$U^0 = [\mathbf{u}^0, (\partial\mathbf{u}^0/\partial x), (\partial\mathbf{u}^0/\partial z), \mathbf{v}^0, (\partial\mathbf{v}^0/\partial x), (\partial\mathbf{v}^0/\partial z)] \quad ,$$

into eq. (7) with relations (A-1) to (A-6) to obtain the following dispersion equation

$$\mathrm{Det}(e^{i\gamma}\mathbf{I}_6 - \mathbf{G}) = 0 \quad . \tag{C-2}$$

where $\gamma = \omega_{num}\Delta t$, $i = \sqrt{(-1)}$, **G** is the same as that presented in eq. (B-2) and $\mathbf{I}_6$ is a sixth-order identity matrix.

For convenience, we suppose $c_{num} = \omega_{num}/k$, $\bar{k} = 2\pi/\lambda$, $\alpha = c\Delta t/h$, $S = h/\lambda$, $\xi = \bar{k}h\cos\theta$, and $\eta = \bar{k}h\sin\theta$. By solving the dispersion equation (C-2), we can get the following ratio of the numerical velocity (c_{num}) to the exact velocity (c_0)

$$R = c_{num}/c_0 = \gamma/2\pi\alpha S \quad , \tag{C-3}$$

where γ satisfies eq. (C-2), which is a nonlinear function with respect to α and S.